Published in final edited form as:
*Syst Biol Reprod Med*. 2010 February ; 56(1): 62–73. doi:10.3109/19396360903469307.

# ERK and AKT Activation at Mid-Gestation and Near-Term in an Ovine Model of Intrauterine Growth Restriction

**Juan A. Arroyo**[a], **Russell V. Anthony**[b], **Thomas A. Parker**[b], and **Henry L. Galan**[a]

[a]Division of Perinatal Medicine in the Department of Obstetrics & Gynecology, University of Colorado and Health Sciences Center in Aurora, CO

[b]Division of Perinatal Medicine in the Department of Pediatrics, University of Colorado and Health Sciences Center in Aurora, CO

## Abstract

Our objective was to determine the relationship between p-ERK, p-AKT, eNOS and NO concentrations in the placenta, uterine and umbilical vessels at mid-gestation and near-term in an ovine model of placental insufficiency and IUGR (PI-IUGR). Eight pregnant ewes were exposed to hyperthermic conditions for either 55 or 80 days to induce IUGR and 8 were used as controls. Sheep necropsies were performed at mid-gestation and near-term for collection of placentomes, umbilical vessels, and uterine artery. These tissues were assessed for eNOS mRNA and protein, and p-ERK and p-AKT protein and compared between groups. Blood was collected for NO determination at the time of necropsy. PI-IUGR pregnancies demonstrated: 1) reduced placental weight at mid-gestation and reduced placental and fetal weight near-term, 2) no changes in eNOS protein concentration in the uterine artery and umbilical vessels, but an increase in NO in umbilical vein blood at both time points, 3) no significant changes in signal transduction makers (ERK/AKT) in placental tissue at mid-gestation but a significant increase near-term in cotyledon tissues, and 4) an increase in p-AKT in the uterine vessels at term. The near-term findings of increased placental p-ERK and p-AKT proteins and umbilical vein NO concentration suggest one mechanism responsible for the increase in placental eNOS previously described in this PI-IUGR model characterized by fetal systemic hypertension and abnormal umbilical artery Doppler velocimetry.

### Keywords

ERK; AKT; NO; eNOS; IUGR; Ovine

## Introduction

Intrauterine growth restriction (IUGR) is an obstetric complication known to increase the risk for fetal and infant morbidity and mortality (Bernstein, Horbar, Badger, Ohlsson, & Golan, 2000; Seeds & Peng, 1998). This disease is associated with the development of long-term adverse health problems for the newborn and adult (Barker, 1993; Barker et al., 1993; Bernstein et al., 2000; Seeds et al., 1998). While there are a number of causes of IUGR, abnormal placentation with placental insufficiency is the most common affecting 3-5% of all pregnancies (Kingdom, Huppertz, Seaward, & Kaufmann, 2000). During pregnancy there is

*Corresponding Author*: Juan A. Arroyo, PhD., Assistant Professor, Department of Obstetrics and Gynecology, University of Colorado Health Sciences Center, Mail Stop B198-5, Academic Office 1, 12631 East 17th Avenue, Room 4001, Aurora, CO 80045, Phone: (303) 724-2032; Fax:(303) 724-2054, juan.arroyo@uchsc.edu.

significant elevation of blood flow through the uterus and placenta in order to meet the demands of the growing fetus (Reynolds & Redmer, 2001). Disruptions in vasoactive modulators such as nitric oxide (NO) are known to be present during IUGR (Myatt, Brewer, & Brockman, 1991; Myatt, Eis, Brockman, Greer, & Lyall, 1997; Thaete, Dewey, & Neerhof, 2004). NO is a potent vasodilator synthesized by the enzyme endothelial nitric oxide synthase (eNOS) and is known to regulate placental blood flow (Myatt et al., 1991; Myatt et al., 1997). In an ovine model of placental insufficiency and IUGR (PI-IUGR) induced with hyperthermic (HT) exposure, placental and umbilical artery eNOS protein is decreased at mid-gestation in the placenta, but increased near-term (Arroyo, Anthony, Parker, & Galan, 2006; Galan et al., 2001). These eNOS data provide some mechanistic explanation for the reduced blood flow, hypertension and increased resistance to blood flow that is characteristic of the HT ovine IUGR fetus (Galan et al., 1999; Galan et al., 1998; Galan et al., 2001). However, the effect on NO concentration and the signaling mechanisms remain unknown.

The extracellular signal-regulated kinase 1/2 (ERK1/2) and the protein kinase B (AKT) pathways are found in many cells types playing various roles. These signaling proteins have not been determined in our model of IUGR but they had been shown to be decreased in other models of IUGR (Ain, Canham, & Soares, 2005).

Our ovine model of PI-IUGR has numerous features characteristic of IUGR in humans, including asymmetrical fetal growth with an increase in umbilical Doppler velocimetry indices and systemic blood pressure, as well as a reduction of placental size (Bell, Wilkening, & Meschia, 1987; Galan et al., 1999; Galan et al., 2001; Thureen, Trembler, Meschia, Makowski, & Wilkening, 1992). IUGR has been induced by a variety of techniques including uterine artery ligation, umbilical artery ligation, nutritional restriction, hypoxia, high altitude exposure, hyperthermic exposure, carunculectomy, caruncle embolization and administration of vasoactive agents (Block, Llanos, & Creasy, 1984; Galan et al., 1998; Giles, Trudinger, Stevens, Alexander, & Bradley, 1989; Molnar & Hertelendy, 1992; Ogata, Swanson, Collins, & Finley, 1990; Skarsgard et al., 2001; Thureen et al., 1992; Wilkening & Meschia, 1991; Yallampalli & Garfield, 1993). Sheep exposed to high ambient temperature throughout pregnancy develop the most severe IUGR (Bell, McBride, Slepetis, Early, & Currie, 1989; Bell et al., 1987; Molnar et al., 1992; Ross, Fennessey, Wilkening, Battaglia, & Meschia, 1996; Thureen et al., 1992). In the present study our goal was to determine underlying mechanisms for the altered eNOS protein concentration by assessing different end points in placental, umbilical and uterine tissues. We chose to study this model to further define the molecular mechanisms related to eNOS and signaling proteins not previously defined in IUGR. In addition, using this model enabled us to define these mechanisms earlier in pregnancy in a controlled fashion that is not achievable in humans. We chose to study these tissues at two time points, mid-gestation (95 days of gestation; dGA) and near-term (130 dGA), two important time points in ovine pregnancy relative to fetal and placental growth. To accomplish this goal we set forth the following objectives comparing HT treated animals and controls: 1) to asses eNOS mRNA and protein concentration at mid-gestation in the uterine and umbilical vessel, 2) to determine the NO concentration in the blood from the umbilical and uterine circulations, and 3) to determine the activation (phosphorylation) of ERK (p-ERK) and AKT (p-AKT) in the placenta and uterine and umbilical vessels.

## Results

Gestational ages, fetal and placental weights are shown in Table 1. Gestational ages of animals were not significantly different between control and PI-IUGR pregnancies at each time point. At mid-gestation, PI-IUGR pregnancies showed a significant decrease in

placental weight (2.4-fold; 440±50 vs. 186±18; p<0.004), but not fetal weight. However, near-term there was a significant decrease in both placental (2.0-fold; 348.7±21.02 vs. 168.7±43.2; p≤0.004) and fetal (1.8-fold; 2914±201g vs. 1718±433g; p≤0.008) weights in the PI-IUGR pregnancies. Hemodynamics and blood gas analysis is shown in Table 2. There was a significant increase in S/D ratios (1.0-fold 3.0±0.34 vs. 3.8±0.18) and systemic blood pressure (1.3-fold 41±1.53mmHg vs. 44.3±1.71mmHg) associate with IUGR pregnancies near-term. There was a significant decrease in fetal O2 saturation and partial pressure of oxygen associated with IUGR pregnancies at this gestational age. There were no pregnancy losses in our studies.

## eNOS mRNA and protein concentrations

**Umbilical vein—**Umbilical vein eNOS mRNA concentration was similar between groups at mid-gestation (Figure 1A) or near-term (Figure 1B). Western blot results for eNOS in the umbilical vein at mid-gestation is shown in figure 1C demonstrating no differences in eNOS protein in the umbilical vein during IUGR.

**Umbilical artery—**Umbilical artery eNOS mRNA or protein concentration did not show any significant difference at mid-gestation in treated animals as compared to controls (Figure 2A and C). A 2.8-fold decrease in eNOS mRNA concentration was observed in the umbilical artery of treated animals near-term (Figure 2B).

**Uterine artery—**Uterine artery eNOS mRNA did not show any difference with treatment at mid-gestation or near-term (Figure 3A and B). Western blot analysis for eNOS in the uterine artery did not show any differences for this protein in IUGR animals as compared to controls (Figure 3C).

## NO determination

Nitric oxide concentration was significantly increased in the blood from the umbilical vessels at mid-gestation in treated animals as compared to controls (Figure 4A). Uterine artery blood analysis did not show any significant differences for NO at this gestational period. Near-term NO in the umbilical vein blood alone was increased in PI-IUGR pregnancies. Neither the uterine or umbilical artery showed significant changes in NO with treatment at this point (Figure 4B).

## Placental ERK and AKT assessment

A characteristic western for AKT and ERK is shown in Figure 5. No significant differences for p-ERK and p-AKT were observed in the placental caruncle (maternal compartment) as compared to controls (Figure 5A and B) at either gestational period studied. Cotyledon tissues (fetal side) showed no significant differences for p-ERK or p-AKT at mid-gestation (Figure 5C). A 1.8-fold increase (p<0.01) in p-ERK and a 2.4-fold increase (p<0.02) for p-AKT were observed in this tissue near-term (Figure 5D).

## Umbilical and Uterine Vessels ERK and AKT assessment

A characteristic western for AKT and ERK is shown in top of Figure 6.

**Umbilical vein—**At mid-gestation, PI-IUGR pregnancies showed a significant 2.3-fold increase (p<0.002) in p-ERK in the umbilical veins with no differences in p-AKT (Figure 6A). In contrast, near-term, the umbilical vein showed no significant differences for p-ERK and p-AKT with treatment as compared to controls (Figure 6B)

**Umbilical artery—**No significant differences were observed in p-ERK and p-AKT within the umbilical artery (Figure 6C) at mid-gestation. In contrast, the umbilical artery exhibited a significant 14.2 fold decrease in p-AKT in near-term PI-IUGR pregnancies (Figure 6D).

**Uterine artery—**No differences for p-ERK and p-AKT were detected between groups in the uterine artery tissues at mid-gestation (Figure 6E), while there was a 4.3 fold increase ($p<0.03$) for p-AKT and no differences in p-ERK at near-term in the sheep PI-IUGR pregnancies (Figure 6F).

## Discussion

We studied two important time points in ovine pregnancy, mid-gestation, when placental growth is at its peak, and near-term when fetal growth is at its maximum. In our study, we found that PI-IUGR placental weights were significantly decreased at both gestational periods as previously reported (Arroyo et al., 2006; Galan et al., 2001). Interestingly, fetal weight was only significantly decreased near-term and not at mid-gestation in the PI-IUGR pregnancies, a finding likely related to the fact that at mid-gestation the fetus is just entering the exponential portion of the fetal growth curve thus making it more difficult to detect differences in growth.

Table 3 summarizes the eNOS, NO, p-AKT and p-ERK results from this study and the eNOS data from the previous studies in cotyledon and caruncles tissues (Arroyo et al., 2006;Galan et al., 2001). NO and eNOS were studied because they are important regulators of vessel vasodilation. In the present study, no significant differences were observed in eNOS mRNA and protein concentration in the umbilical vein, umbilical artery or uterine artery of HT animals at mid-gestation. Near-term, only umbilical artery eNOS mRNA was significantly decreased which is consistent with the findings of a decrease in eNOS protein level previously obtained in this vessel at this gestational period (Arroyo et al., 2006). These results suggest a eNOS is transcriptionally regulated in these vessels in this model of IUGR. NO was increased in the serum from the umbilical vein at both mid-gestation and near-term gestational points. In contrast, serum NO was only increased in the umbilical artery at mid-gestation while there was no change observed for serum NO from the uterine artery at any gestational period. The general lack of eNOS changes in the umbilical artery and uterine artery is understandable as these are conduit, not resistance vessels. The finding of an increase NO in the blood from the umbilical vein is likely due to transfer of NO produced upstream in the cotyledon where eNOS protein is increased (Arroyo et al., 2006).

For the placental signaling studies, the placentomes were separated into caruncles and cotyledons reflecting the maternal and fetal sides of the placenta, respectively. Placental eNOS experiments were not repeated as this data has been published previously. In studies that assess important signaling proteins such as AKT and ERK, it is common to find only one or the other that is affected and, as such, both are commonly studied simultaneously (Boyd et al., 2003; Dimmeler, Assmus, Hermann, Haendeler, & Zeiher, 1998; Jo et al., 1997; Sumpio et al., 2005; Tseng, Peterson, & Berk, 1995). At mid-gestation, the cotyledon (fetal side) did not show any differences in p-AKT or p-ERK as compared to controls. In contrast, our near-term studies showed increases in both of these proteins. There was no change in p-ERK or p-AKT in the maternal side of the placenta (caruncle). This is similar to lack of change in other proteins in the caruncle related to vasoregulation such as eNOS and VEGF (Arroyo et al., 2006; Galan et al., 2001; Regnault et al., 2003). This is consistent with the idea that hyperthermic exposure and IUGR in our model has its primary effect on the fetal side of the placenta.

Since the near-term HT PI-IUGR ovine pregnancy model demonstrates reduced absolute uterine and umbilical (ml/min) blood flows, increased umbilical artery Doppler velocimetry indices (Galan et al., 1998) and fetal systemic hypertension (Galan et al., 2005), we also chose to study the uterine artery and umbilical vessels for activation of ERK and AKT anticipating that there may be alterations in their protein concentration. At mid-gestation, umbilical veins of PI-IUGR pregnancies showed a significant increase in p-ERK, but not p-AKT, and no significant differences in the uterine or umbilical artery expression of p-ERK or p-AKT. In the near-term HT pregnancies, no differences were observed for either protein in the umbilical veins, which may again be explained by the primary conduit functions of these vessels.

It is natural to draw associations and to speculate what these findings represent relative to what is known in the HT-induced model of IUGR. Several characteristics of this IUGR model suggest marked disruption of normal vascular development and disregulation as indicated by a variety of molecular and physiologic parameters such as increased umbilical artery Doppler velocimetry (e.g. increased impedance to placental blood flow) and fetal hypertension (Galan et al., 2005; Galan et al., 1998). These physiologic findings are easy to understand when viewing the abnormal vascular casts of the villous tree in this model (Regnault, Galan, Parker, & Anthony, 2002). VEGF, eNOS, and Angiopoitein 2 abnormalities in the cotyledon provide molecular support for abnormal vascular development and function (Arroyo et al., 2006; Galan et al., 2001; Hagen, Orbus, Wilkening, Regnault, & Anthony, 2005; Regnault et al., 2003). The current study findings taken collectively with the above past findings provide indirect evidence that shear stress may play a role in vasoregulation in this model of IUGR. Shear stress or the frictional force produced by blood flow is known to modulate physiological and pathological processes in the cells. Some of the processes regulated by shear stress are vascular tone, vessel remodeling, hemostasis and others (Boyd et al., 2003; Davies, Robotewskyj, & Griem, 1994). Shear stress induces eNOS mRNA and protein expression in endothelial cells (Ranjan, Xiao, & Diamond, 1995; Uematsu et al., 1995). Induction of genes by shear stress in endothelial cells is mediated, in part, by ERK and AKT. Western blot of the near-term cotyledon tissues showed a significant increase for both p-ERK and p-AKT in PI-IUGR animals, and shear stress has been shown to be to be a regulator of eNOS activity, p-ERK and p-AKT proteins. This pattern of increased p-AKT and p-ERK, as markers of shear stress, is consistent with the increase in eNOS protein content in the cotyledon of HT IUGR pregnancies (Arroyo et al., 2006; Regnault, Orbus, Battaglia, Wilkening, & Anthony, 1999).

Our previous placental and umbilical and uterine vessel eNOS studies (Regnault et al., 2002) lead to the investigation of the activation of ERK and AKT in an ovine model of IUGR. ERK pathway is involved in cellular proliferation and differentiation in the cells and this protein is phosphorylated during shear stress in endothelial cells (Azuma et al., 2001; Azuma et al., 2000; Sumpio et al., 2005). AKT protein is similarly phosphorylated by shear stress in endothelial cells (Dimmeler et al., 1998; Kudo et al., 2005; Wedgwood, Mitchell, Fineman, & Black, 2003; Wyatt, Steinert, & Mann, 2004). Dimmeler et al (1998) demonstrated that eNOS activation is mediated by the phosphorylation of AKT in cultured endothelial cells, thus demonstrating a link between eNOS and AKT activation (Dimmeler et al., 1998). While we speculate for current and past studies that shear stress is a possible mechanism for the increased placental eNOS seen at term, we also recognize that there are other mechanisms that regulate eNOS and the signaling molecules ERK and AKT. An association between eNOS, NO and p-AKT and p-ERK in IUGR has not been previously shown and collectively serve as surrogate markers of shear stress in this model of PI-IUGR with umbilical artery Doppler abnormalities and fetal systemic hypertension. In vitro pharmacologic studies are underway to better understand potential mechanisms for the altered shear stress and vasoreactivity suspected in this model of IUGR.

## Materials and Methods

### Animal care

This study was approved by the University of Colorado Health Sciences Center Animal Care and Use Committee. Mixed-breed (Columbia-Rambouillet) ewes with time-dated singleton pregnancies (total of 16 animals) were used for this study. Ewes were exposed to environmental conditions as previously described (Regnault et al., 1999; Thureen et al., 1992) and consisted of the following: (1) temperature maintained at 40°C for 12 hours during the day and decreased to 35°C at night; (2) humidity was kept between 35% and 40%. Animals were separated into two groups based on length of HT exposure and gestational age at necropsy. In the first group, four ewes were housed in the environmental chamber for 55 days beginning at 40 dGA (term=147 days) and four ewes were housed at ambient temperature (20 ± 2 °C) to serve as controls. These animals underwent necropsy at 95 days of gestation (dGA; mid-gestation). In the second group, four ewes were exposed to HT conditions for 80 days (near-term) and were removed to control conditions at approximately 120 days gestation. And additional four ewes were kept at ambient temperature to use as controls. All animals in this group were euthanized at 130 dGA. All ewes were pair-fed and offered water ad libitum. At the time of necropsy, prior to euthanasia, blood was collected form the uterine and umbilical vessels by cordocentesis. Following euthanasia, fetal and placentome weights were recorded. The placentomes were separated into cotyledon (fetal) and caruncle (maternal) components, and frozen in liquid nitrogen for western blot analysis. Uterine artery and umbilical vessels were excised and dissected carefully from each other and frozen in liquid nitrogen for protein analysis.

### RNA Extraction and cDNA synthesis

RNA was extracted from the collected tissues using the TRI REAGENT method. 100 mg of tissues were homogenized in 1 ml of TRI REAGENT (Sigma, Saint Louis, MO). Samples were centrifuged, chloroform extracted, precipitated and washed in cold 75% ethanol. Samples were purified using a Qiagen RNeasy Mini Kit (Qiagen, Valencia, CA). cDNA was produced through reverse transcription using the First-Strand cDNA Synthesis protocol from the SuperScript III kit by Invitrogen (Invitrogen, Carlsbad, CA). 5 μg of total RNA was mixed with 50 μM of oligo (dT) primers, 10 mM dNTP mix and DEPC-treated water. Samples were incubated at 65°C for 5 min. and then placed on ice for at least 1 min. Ten μl of cDNA Synthesis mix (10x RT buffer, 25 mM $MgCl_2$, 0.1 M DTT, RNase out and SuperScript III RT) was added to each sample and then incubated at 50°C for 60 min. Reactions were terminated by incubation at 70°C for 15 min. RNase H (1 μl) was added to each sample and then incubated at 37 °C for 20 min. Samples were stored at −20°C until needed.

### Real Time PCR

Quantitative Real Time PCR was used to quantify eNOS mRNA concentrations in our samples. Each sample cDNA (10ng) was used for real time PCR using our Ovine eNOS forward (5′-TGC ATG ACA TTG AGA GCA AAG GGC -3′) and ovine eNOS reverse (5′-ATG TCC TCG TGA TAG CGT TGC TGA -3′), and compared to a standard curve generated by known quantities of eNOS cDNA to determine starting quantity. To normalize our eNOS data, sample cDNA were subjected to real-time PCR using primers (forward 5′-TCA ACC AGG TGG AGA TCA ACG -3′ and reverse 5′-TGC TTT ACG GGC TTG TAG GTG -3′) for ribosomal protein S15, and a standard curve of known quantities of S15 cDNA. The amplification efficiencies were 98% and 99% for eNOS and S15, respectively.

### Western blot analysis

Vessel, cotyledon and caruncle tissues were homogenized in protein lysis buffer and proteins were separated on a 10% SDS-PAGE and western blot for eNOS was performed as previously described by Arroyo et al (2006). Western blot was also performed using antibodies against rabbit p-ERK, ERK, p-AKT, or AKT (dilution of 1:500; Cell signalling, Dancers, MA). Caruncles and cotyledons were not assessed for eNOS protein as it has been previously published (Arroyo et al., 2006; Galan et al., 2001; Thaete, Neerhof, & Caplan, 1997). A secondary anti-rabbit IgG-HRP antibody (dilution 1:5,000; Cell signalling, Dancers, MA) was incubated for 1 hour at room temperature. The membranes were rinsed and incubated with chemiluminescent substrate (Pierce, Rockford, IL) for 5 min. The emission of light was detected using x-ray film. Each membrane was stripped of antibodies and reprobed utilizing antibody against mouse beta-actin (dilution 1:4,000; MP Biomedicals, Aurora, OH) to confirm loading consistencies in each lane. Presence of these proteins was confirmed by densitometry and quantified. Results were compared to the untreated controls.

### NO determination

Uterine artery and umbilical vessel blood samples were collected prior to euthanization. Protocol was followed as suggested by the manufacturer (Assay Designs, Ann Arbor, Michigan). Briefly, blood samples were ultrafiltrated through a 10,000 MWCO filter. After filtration, a solution of NADH was added to the samples followed by the addition of the Nitrate Reductase solution. Samples were incubated at 37°C for 30 min. After incubation, the Griess reagents were added and samples were incubated for 10 min at room temperature. The optical densities of the samples were determined at 540-570 nm.

### Statistical analysis

Comparisons of the following end-points were made between control and PI-IUGR pregnancies: fetal and placental weights, eNOS mRNA and protein concentration, NO production and p-ERK and p-AKT western blot analysis. Treatment effects were determined using Mann-Whitney test with $p<0.05$ considered significant.

## Acknowledgments

We will like to thank Bradley Ziebell for the technical assistance he rendered.

This study was supported by the NIH grant R01 HL071990.

## References

Ain R, Canham LN, Soares MJ. Dexamethasone-induced intrauterine growth restriction impacts the placental prolactin family, insulin-like growth factor-II and the Akt signaling pathway. J Endocrinol 2005;185:253–63. [PubMed: 15845918]

Arroyo JA, Anthony RV, Parker TA, Galan HL. Differential expression of placental and vascular endothelial nitric oxide synthase in an ovine model of fetal growth restriction. Am.J.Obstet.Gynecol 2006;195:771–777. [PubMed: 16875646]

Azuma N, Akasaka N, Kito H, Ikeda M, Gahtan V, Sasajima T, Sumpio BE. Role of p38 MAP kinase in endothelial cell alignment induced by fluid shear stress. Am.J.Physiol Heart Circ.Physiol 2001;280:H189–H197. [PubMed: 11123233]

Azuma N, Duzgun SA, Ikeda M, Kito H, Akasaka N, Sasajima T, Sumpio BE. Endothelial cell response to different mechanical forces. J.Vasc.Surg 2000;32:789–794. [PubMed: 11013043]

Barker DJ. The intrauterine origins of cardiovascular disease. Acta Paediatr Suppl 1993;82(Suppl 391):93–99. [PubMed: 8219485]

Barker DJ, Gluckman PD, Godfrey KM, Harding JE, Owens JA, Robinson JS. Fetal nutrition and cardiovascular disease in adult life. Lancet 1993;341:938–941. [PubMed: 8096277]

Bell AW, McBride BW, Slepetis R, Early RJ, Currie WB. Chronic heat stress and prenatal development in sheep: I. Conceptus growth and maternal plasma hormones and metabolites. J.Anim Sci 1989;67:3289–3299. [PubMed: 2613577]

Bell AW, Wilkening RB, Meschia G. Some aspects of placental function in chronically heat-stressed ewes. J Dev Physiol 1987;9:17–29. [PubMed: 3559063]

Bernstein IM, Horbar JD, Badger GJ, Ohlsson A, Golan A, The Vermont Oxford Network. Morbidity and mortality among very-low-birth-weight neonates with intrauterine growth restriction. Am.J.Obstet.Gynecol 2000;182:198–206. [PubMed: 10649179]

Block BS, Llanos AJ, Creasy RK. Responses of the growth-retarded fetus to acute hypoxemia. Am J Obstet Gynecol 1984;148:878–85. [PubMed: 6711629]

Boyd NL, Park H, Yi H, Boo YC, Sorescu GP, Sykes M, Jo H. Chronic shear induces caveolae formation and alters ERK and Akt responses in endothelial cells. Am.J.Physiol Heart Circ.Physiol 2003;285:H1113–H1122. [PubMed: 12763750]

Davies PF, Robotewskyj A, Griem ML. Quantitative studies of endothelial cell adhesion. Directional remodeling of focal adhesion sites in response to flow forces. J.Clin.Invest 1994;93:2031–2038. [PubMed: 8182135]

Dimmeler S, Assmus B, Hermann C, Haendeler J, Zeiher AM. Fluid shear stress stimulates phosphorylation of Akt in human endothelial cells: involvement in suppression of apoptosis. Circ.Res 1998;83:334–341. [PubMed: 9710127]

Galan HL, Anthony RV, Rigano S, Parker TA, de Vrijer B, Ferrazzi E, Wilkening RB, Regnault TR. Fetal hypertension and abnormal Doppler velocimetry in an ovine model of intrauterine growth restriction. Am J Obstet Gynecol 2005;192:272–279. [PubMed: 15672036]

Galan HL, Hussey MJ, Barbera A, Ferrazzi E, Chung M, Hobbins JC, Battaglia FC. Relationship of fetal growth to duration of heat stress in an ovine model of placental insufficiency. Am J Obstet Gynecol 1999;180:1278–1282. [PubMed: 10329890]

Galan HL, Hussey MJ, Chung M, Chyu JK, Hobbins JC, Battaglia FC. Doppler velocimetry of growth-restricted fetuses in an ovine model of placental insufficiency. Am J Obstet Gynecol 1998;178:451–456. [PubMed: 9539507]

Galan HL, Regnault TR, Le Cras TD, Tyson RW, Anthony RV, Wilkening RB, Abman SH. Cotyledon and binucleate cell nitric oxide synthase expression in an ovine model of fetal growth restriction. J Appl Physiol 2001;90:2420–2426. [PubMed: 11356809]

Giles WB, Trudinger BJ, Stevens D, Alexander G, Bradley L. Umbilical artery flow velocity waveform analysis in normal ovine pregnancy and after carunculectomy. J.Dev.Physiol 1989;11:135–138. [PubMed: 2681386]

Hagen AS, Orbus RJ, Wilkening RB, Regnault TR, Anthony RV. Placental expression of angiopoietin-1, angiopoietin-2 and tie-2 during placental development in an ovine model of placental insufficiency-fetal growth restriction. Pediatr Res 2005;58:1228–1232. [PubMed: 16306198]

Jo H, Sipos K, Go YM, Law R, Rong J, McDonald JM. Differential effect of shear stress on extracellular signal-regulated kinase and N-terminal Jun kinase in endothelial cells. Gi2- and Gbeta/gamma-dependent signaling pathways. J.Biol.Chem 1997;272:1395–1401. [PubMed: 8995450]

Kingdom J, Huppertz B, Seaward G, Kaufmann P. Development of the placental villous tree and its consequences for fetal growth. Eur J Obstet Gynecol Reprod Biol 2000;92:35–43. [PubMed: 10986432]

Kudo FA, Warycha B, Juran PJ, Asada H, Teso D, Aziz F, Frattini J, Sumpio BE, Nishibe T, Cha C, Dardik A. Differential responsiveness of early- and late-passage endothelial cells to shear stress. Am.J.Surg 2005;190:763–769. [PubMed: 16226955]

Molnar M, Hertelendy F. N omega-nitro-L-arginine, an inhibitor of nitric oxide synthesis, increases blood pressure in rats and reverses the pregnancy-induced refractoriness to vasopressor agents. Am J Obstet Gynecol 1992;166:1560–1567. [PubMed: 1595813]

Myatt L, Brewer A, Brockman DE. The action of nitric oxide in the perfused human fetal-placental circulation. Am J Obstet Gynecol 1991;164:687–692. [PubMed: 1899534]

Myatt L, Eis AL, Brockman DE, Greer IA, Lyall F. Endothelial nitric oxide synthase in placental villous tissue from normal, pre-eclamptic and intrauterine growth restricted pregnancies. Hum.Reprod 1997;12:167–172. [PubMed: 9043923]

Ogata ES, Swanson SL, Collins JW Jr. Finley SL. Intrauterine growth retardation: altered hepatic energy and redox states in the fetal rat. Pediatr.Res 1990;27:56–63. [PubMed: 2296473]

Ranjan V, Xiao Z, Diamond SL. Constitutive NOS expression in cultured endothelial cells is elevated by fluid shear stress. Am.J.Physiol 1995;269:H550–H555. [PubMed: 7544542]

Regnault TR, de VB, Galan HL, Davidsen ML, Trembler KA, Battaglia FC, Wilkening RB, Anthony RV. The relationship between transplacental O2 diffusion and placental expression of PlGF, VEGF and their receptors in a placental insufficiency model of fetal growth restriction. J.Physiol 2003;550:641–656. [PubMed: 12740423]

Regnault TR, Galan HL, Parker TA, Anthony RV. Placental development in normal and compromised pregnancies--a review. Placenta 2002;23(Suppl A):S119–29. [PubMed: 11978069]

Regnault TR, Orbus RJ, Battaglia FC, Wilkening RB, Anthony RV. Altered arterial concentrations of placental hormones during maximal placental growth in a model of placental insufficiency. J Endocrinol 1999;162:433–442. [PubMed: 10467235]

Reynolds LP, Redmer DA. Angiogenesis in the placenta. Biol.Reprod 2001;64:1033–1040. [PubMed: 11259247]

Ross JC, Fennessey PV, Wilkening RB, Battaglia FC, Meschia G. Placental transport and fetal utilization of leucine in a model of fetal growth retardation. Am.J.Physiol 1996;270:E491–E503. [PubMed: 8638698]

Seeds JW, Peng T. Impaired growth and risk of fetal death: is the tenth percentile the appropriate standard? Am.J.Obstet.Gynecol 1998;178:658–669. [PubMed: 9579427]

Skarsgard ED, Amii LA, Dimmitt RA, Sakamoto G, Brindle ME, Moss RL. Fetal therapy with rhIGF-1 in a rabbit model of intrauterine growth retardation. J.Surg.Res 2001;99:142–146. [PubMed: 11421616]

Sumpio BE, Yun S, Cordova AC, Haga M, Zhang J, Koh Y, Madri JA. MAPKs (ERK1/2, p38) and AKT can be phosphorylated by shear stress independently of platelet endothelial cell adhesion molecule-1 (CD31) in vascular endothelial cells. J.Biol.Chem 2005;280:11185–11191. [PubMed: 15668248]

Thaete LG, Dewey ER, Neerhof MG. Endothelin and the regulation of uterine and placental perfusion in hypoxia-induced fetal growth restriction. J Soc Gynecol Investig 2004;11:16–21.

Thaete LG, Neerhof MG, Caplan MS. Endothelin receptor A antagonism prevents hypoxia-induced intrauterine growth restriction in the rat. Am J Obstet Gynecol 1997;176:73–6. [PubMed: 9024092]

Thureen PJ, Trembler KA, Meschia G, Makowski EL, Wilkening RB. Placental glucose transport in heat-induced fetal growth retardation. Am.J.Physiol 1992;263:R578–R585. [PubMed: 1415644]

Tseng H, Peterson TE, Berk BC. Fluid shear stress stimulates mitogen-activated protein kinase in endothelial cells. Circ.Res 1995;77:869–878. [PubMed: 7554140]

Uematsu M, Ohara Y, Navas JP, Nishida K, Murphy TJ, Alexander RW, Nerem RM, Harrison DG. Regulation of endothelial cell nitric oxide synthase mRNA expression by shear stress. Am.J.Physiol 1995;269:C1371–C1378. [PubMed: 8572165]

Wedgwood S, Mitchell CJ, Fineman JR, Black SM. Developmental differences in the shear stress-induced expression of endothelial NO synthase: changing role of AP-1. Am.J.Physiol Lung Cell Mol.Physiol 2003;284:L650–L662. [PubMed: 12533439]

Wilkening RB, Meschia G. Effect of occluding one umbilical artery on placental oxygen transport. Am.J.Physiol 1991;260:H1319–H1325. [PubMed: 1901461]

Wyatt AW, Steinert JR, Mann GE. Modulation of the L-arginine/nitric oxide signalling pathway in vascular endothelial cells. Biochem.Soc.Symp 2004:143–156. [PubMed: 15777019]

Yallampalli C, Garfield RE. Inhibition of nitric oxide synthesis in rats during pregnancy produces signs similar to those of preeclampsia. Am J Obstet Gynecol 1993;169:1316–20. [PubMed: 8238200]

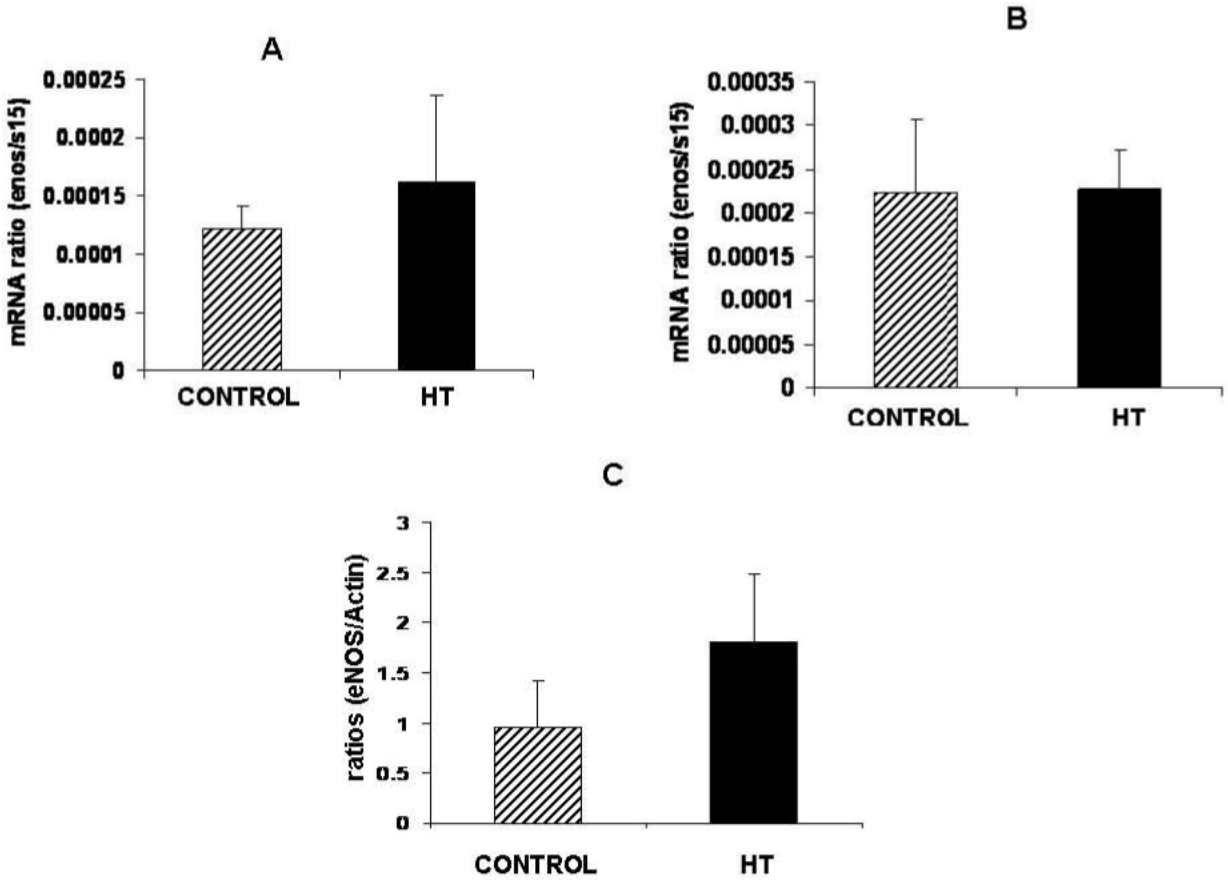


**Figure 1.**

eNOS protein and mRNA in the umbilical vein during IUGR. No significant differences were observed for eNOS mRNA in the umbilical vein at mid-gestation (A) and near-term (B) in treated animals vs. controls. A non-significant increase (1.9-fold) in eNOS protein expression was observed for the umbilical vein at mid-gestation during heat induced IUGR in the sheep (C).

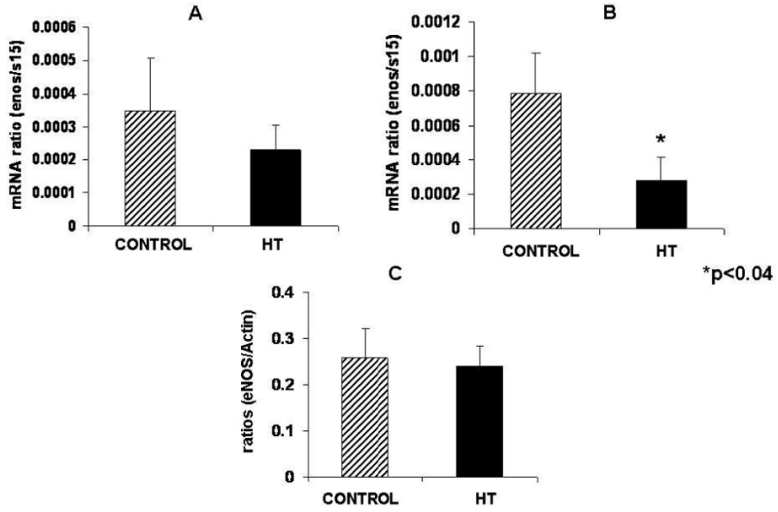


**Figure 2.**

Umbilical artery eNOS protein did not change at mid-gestation during IUGR in the sheep. Umbilical artery eNOS mRNA concentration was not change at mid-gestation (A) while a significant decrease was observed for eNOS mRNA in this tissue with treatment near-term (B). eNOS protein is not affected in the umbilical artery of treated animals as compared to controls (C).

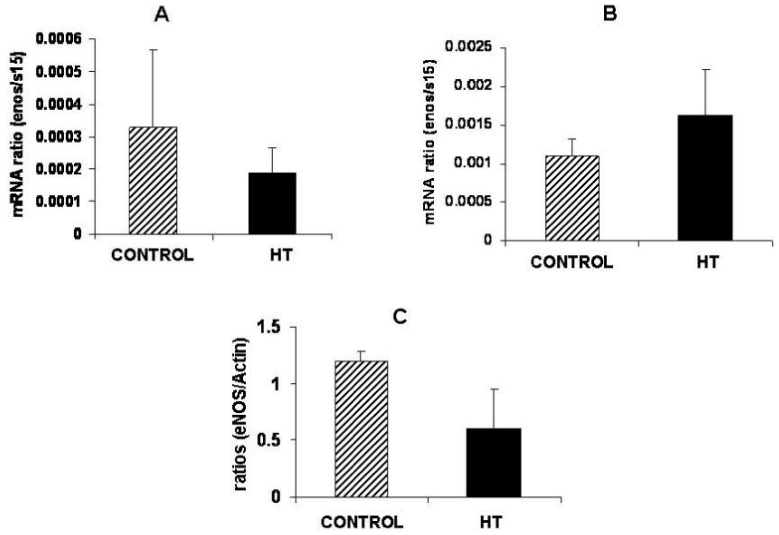


**Figure 3.**

eNOS protein is decreased in the uterine artery of IUGR animals. No significant differences were observed for eNOS mRNA concentration in the uterine artery of treated animals at mid-gestation (A) and near-term (B). A 2.0-fold non-significant decrease was observed for eNOS protein in the uterine artery of treated animals vs. controls (C).

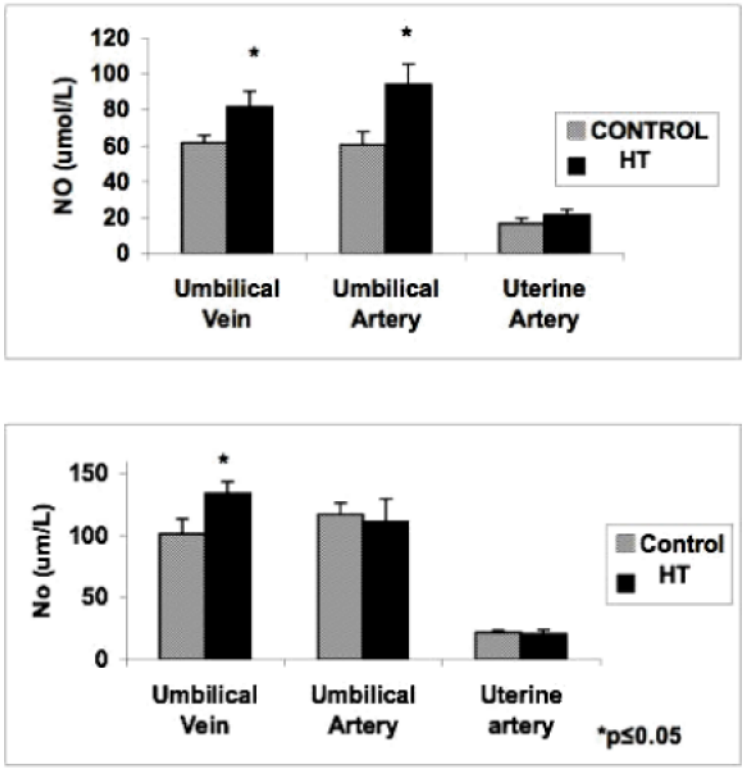


**Figure 4.**
Blood NO concentration in the uterine artery and umbilical vessels of HT treated animals. Nitric oxide was significantly increased in the umbilical vessels at mid- gestation (A). Only the umbilical vein showed a significant increase for NO near-term (B).

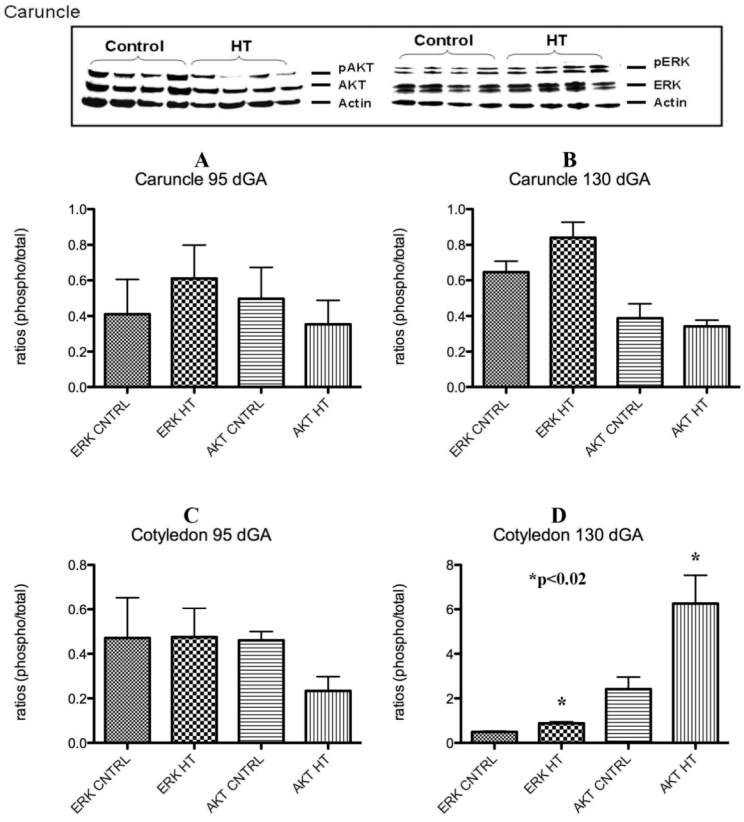


**Figure 5.**

Placental p-ERK and p-AKT during IUGR. A characteristic western for ERK and AKT is shown in top panel of this figure. No significant differences were observed for these proteins in the caruncle at any gestational point studies (A and B). Only a significant increase in p-ERK and p-AKT was observed in the cotyledon near term during HT treatment in the sheep (C and D).

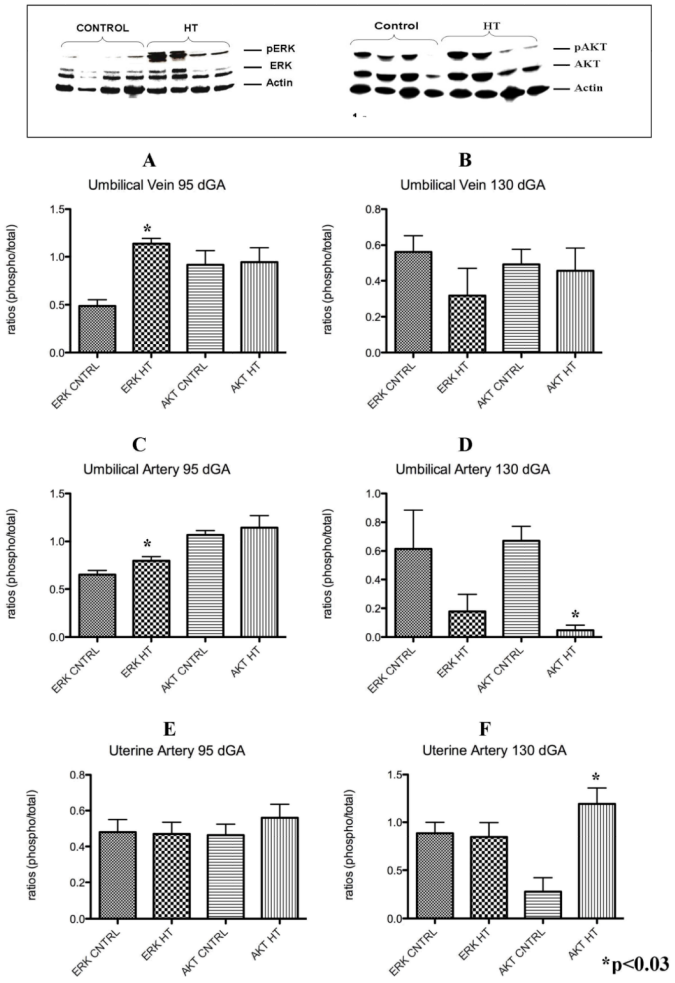


**Figure 6.**

Umbilical vessels and uterine artery p-ERK and p-AKT during IUGR in the sheep. Umbilical vein p-ERK was significantly increased in these vessels at mid-gestation but not near-term in the treated animals vs. controls (A and B). p-ERK was increase at mid-gestation while p-AKT was decreased in the umbilical artery of treated animals during IUGR (C and D). Uterine artery p-AKT was increase only near-term during IUGR (E and F).

**Table 1**

Necropsy age, placental and fetal weights in IUGR and control animals

| | 95 dGA Studies | | | 130 dGA Studies | | |
|---|---|---|---|---|---|---|
| | **HT** | **Control** | **P value** | **HT** | **Control** | **P value** |
| Gestational Age at Necropsy | 96±0.5 | 96.5±0.9 | 0.22 | 131.2±0.6 | 129.4±1.2 | 0.11 |
| Placental Weight (g) | 186±18 | 440±50 | 0.004 | 168.7±43.2 | 348.7±21 | 0.004 |
| Fetal Weight (g) | 682±205 | 715±11 | 0.79 | 1718±433 | 2914±201. | 0.008 |

HT = Hyperthermia

**Table 2**

Near-term Hemodynamic and blood gas results*

| | Control | IUGR | P Value |
|---|---|---|---|
| **Hemodynamic Data** | | | |
| Systemic blood pressure | 41±1.53 mmHg | 44.3±1.71mmHg | 0.026 |
| S/D ratios | 3.0±0.34 | 3.8±0.18 | 0.009 |
| **Blood gas data** | | | |
| pH | 7.37±0.01 | 7.4±0.05 | 0.161 |
| $pO_2$ | 18.9±1.47mmHg | 13.9±1.9mmHg | 0.001 |
| $pCO_2$ | 45.9±4.61mmhg | 50.98±3.95mmHg | 0.06 |
| $O_2$ | 52.2±7.03% | 33.05±10.98% | 0.007 |

* Arroyo et al., 2006

## Table 3

Summary of results obtained in study

| | | Fetal (Cotyledon) | Maternal (Caruncle) |
|---|---|---|---|
| **Mid-gestation** | | | |
| | p-ERK | - | - |
| | p-AKT | - | - |
| | eNOS | ↓ ** | ↓ ** |
| **Near-Term** | | | |
| | p-ERK | ↑ | - |
| | p-AKT | ↑ | - |
| | eNOS | ↑ * | -* |

| | | Umbilical Vein | Umbilical Artery | Uterine artery |
|---|---|---|---|---|
| **Mid-Gestation** | | | | |
| | NO | ↑ | ↑ | - |
| | p-ERK | ↑ | - | - |
| | p-AKT | - | - | - |
| | eNOS | - | - | - |
| **Near-Term** | | | | |
| | NO | ↑ | - | - |
| | p-ERK | - | - | - |
| | p-AKT | - | ↓ | ↑ |
| | eNOS | -* | ↓ * | -* |

↑ = significant increase

↓ = significant decrease

* Arroyo et al., 2006

** Galan et al., 2001